

Construction of Two New 3D Supramolecular Networks with 3-Pyridyl-4-yl-Benzoic Acid Ligands: Synthesis, Characterization, and Luminescence¹

J. Guo^{a, b}, S. J. Li^a, D.-L. Miao^c, J. S. Liu^{a, *}, and W. D. Song^{b, *}

^a School of Environmental Science and Engineering, Donghua University, Shanghai, 200051 P.R. China

^b School of Petroleum & Chemical Engineering, Zhejiang Ocean University, Zhoushan, 316000 P.R. China

^c College of Food Science and Technology, Guangdong Ocean University, Zhanjiang, 524088 P.R. China

*e-mail: liujianshe@dhu.edu.cn; songwd60@126.com

Received April 17, 2012

Abstract—Two new coordination polymers with 3-pyridyl-4-yl-benzoic acid (3,4-HPybz), namely, $[\text{Zn}(3,4-\text{HPybz})_2 \cdot 2\text{H}_2\text{O}]_n$ (**I**) and $[\text{Ag}(3,4-\text{HPybz})(3,4-\text{HPybz})]_n$ (**II**), have been synthesized and characterized by elemental analysis, IR spectroscopy, thermogravimetric analysis, and single crystal X-ray diffraction. Compound **I** crystallizes in the triclinic system and has $P\bar{1}$ space group. Complex **I** is an infinite 1D chain polymer and the infinite chains array uniformly in a 3D supramolecular network which possesses abundant $\text{O}-\text{H}\cdots\text{O}$ hydrogen-bonding interactions among the occupied and unoccupied carboxylate O atoms and the coordinated water molecules; compound **II** crystallizes in the triclinic system and has $P\bar{1}$ space group, **II** is an infinite chain with the repeat sequence of $\text{Ag1(I)}-\text{Ag2(I)}-\text{Ag1(I)}$, in which weak intermolecular interactions play a key role in forming the final 3D supramolecular architectures. The photoluminescences and lifetime of **I** and **II** in the solid state have been investigated.

DOI: 10.1134/S1070328414010011

INTRODUCTION

The past decade has witnessed tremendous progress in the synthesis of metal-organic frameworks and the investigation of their properties. The compounds based on the ligands and metal centers display a great variety of properties, such as molecular recognition, heterogeneous catalysis, ion exchange, magnetic and photochemical areas, as well as their intriguing variety of topologies [1–4]. Generally, the diversity of the framework structures of such materials as the result of the self-assemble process greatly depends on the selection of the metal centers and organic spacers, as well as on the reaction pathways [5]. In addition, weak intermolecular forces in these coordination polymers have been well-studied and can be used to design and synthesize complexes with interesting architectures and functions. The judicious selection of a multifunctional ligand with hydrgoen donors and acceptors and suitable spacers between linking groups to connect metal ions to generate a fascinating configuration is a common strategy.

N-Heterocyclic multicarboxylic acids have been widely used to construct coordination polymers for their potential application. Among the reported frameworks, the multifunctional organic ligands that incorporate both pyridyl and carboxylate groups, such

as 3-pyridyl-3-yl-benzoate and 4-pyridyl-4-yl-benzoate, have been proved to be excellent candidates for constructing novel coordination polymers with different properties [6].

However, their isomeric building block 3-pyridin-4-yl-benzoate has been largely unexplored so far [7, 8]. Four 3D complexes assembled from Mn(II), Zn(II), Cd(II), or Pb(II) with 3,4-Pybz are presented in [9], two isostructural complexes are obtained in [10] and three isostructural complexes are reported and studied the magnetic properties in [11].

We choose the unsymmetrical ligand 3-pyridin-4-yl-benzoic acid (3,4-HPybz) in the self-assembly. Hein, we report two 3D supramolecular networks: $[\text{Zn}(3,4-\text{HPybz})_2 \cdot 2\text{H}_2\text{O}]_n$ (**I**), $[\text{Ag}(3,4-\text{HPybz})(3,4-\text{HPybz})]_n$ (**II**). Complexes **I** and **II** are 1D infinite chains and extended into the final 3D framework via hydrogen bonding and/or $\pi-\pi$ stacking interactions.

EXPERIMENTAL

Materials and measurements. All solvents and reagents were commercially available and used without further purification. Elemental (C, H, and N) analyses were performed on PerkinElmer 240 CHN element analyzer. Infrared (IR) spectra were recorded (4000–400 cm^{-1}) as KBr disks on a Bruker 1600 FTIR spectrometer. Thermogravimetric analysis (TGA) experi-

¹ The article is published in the original.

ments were carried out on a PerkinElmer TG/DTA 6300 system with a heating rate of 10°C/min from room temperature to 600°C under nitrogen atmosphere. Luminescence spectra for crystal solid samples were recorded at room temperature on a Hitachi F-4500 fluorescence spectrophotometer.

Synthesis of complex I. A mixture of $Zn(NO_3)_2 \cdot 6H_2O$ (0.14 g, 0.5 mmol), 3,4-HPybz (0.1 g, 0.5 mmol) and H_2O (10 mL) with pH adjusted to 4 was stirred for 30 min in air. Afterwards, it was sealed in a 20 mL Teflon reactor and kept under autogenous pressure at 150°C for 96 h. The mixture was cooled to room temperature at a rate of 5°C h⁻¹ and colorless plate crystals were obtained in a yield of 51% based on Zn.

For $C_{24}H_{20}N_2O_6Zn$ (**I**)

anal. calcd., %: C, 57.85; H, 4.02; N, 5.62.
Found, %: C, 57.78; H, 4.06; N, 5.63.

IR bands (KBr; ν , cm⁻¹): 3242 s, 1589 s, 1537 vs, 1409 s, 1373 s, 1196 w, 1136 s, 1036 w, 1007 w, 863 s, 779 vs, 708 w, 558 w, 484 w.

Synthesis of complex II. A mixture of $AgNO_3$ (0.09 g, 0.5 mmol), 3,4-Hpybz (0.14 g, 0.5 mmol) and water (15 mL) was stirred for 30 min in air with the pH of 8 adjusted by NaOH, sealed in a 20 mL Teflon reactor and kept under autogenous pressure at 170°C for 72 h. The mixture was cooled to room temperature at a rate of 5°C h⁻¹ and colorless plate crystals were obtained in a yield of 36% based on Ag.

For $C_{24}H_{17}N_2O_4Ag$ (**II**)

anal. calcd., %: C, 57.00; H, 3.36; N, 5.54.
Found, %: C, 56.82; H, 3.33; N, 5.63.

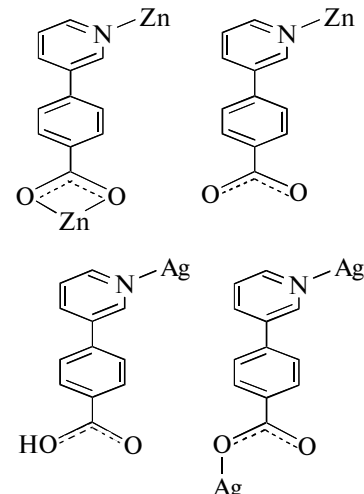
IR bands (KBr; ν , cm⁻¹): 3067 w, 1695 s, 1592 s, 1433 s, 1340 w, 1135 s, 864 s, 812 w, 776 s, 742 w, 705 w, 507 w.

X-ray structure determination. Diffraction data of complexes **I** and **II** were performed on a Bruker SMART CCD 1000 diffractometer operating at 50 kV and 30 mA using MoK_α radiation ($\lambda = 0.71073 \text{ \AA}$) at 298 K. Data collection and reduction were performed using the SMART and SAINT software [12]. Multi-scan absorption correction was applied using the SADABS program [12]. The structures were solved by direct methods and refined by full-matrix least-squares techniques using the SHELXTL program package [13]. All non-hydrogen atoms were treated anisotropically. The hydrogen atoms belonging to C and N atoms were calculated theoretically. The hydrogen atoms of water molecules were located in a difference Fourier maps. Hydrogen atoms on water molecules were located from difference Fourier maps and refined with distance restraints of O—H 0.84(2) Å and H···H 1.39(2) Å. Crystal data and details of the data collection and refinement for two compounds are listed in Table 1. The data for selected bond lengths, an-

gles and hydrogen bonds are listed in Table 2. Supplementary material has been deposited with the Cambridge Crystallographic Data Centre (nos. 857472 (**I**), 857472 (**II**); deposit@ccdc.cam.ac.uk or <http://www.ccdc.cam.ac.uk>).

RESULTS AND DISCUSSION

The asymmetric unit of **I** (Fig. 1a) consists of one Zn^{2+} ion, two 3,4-Pybz ligands and two coordinated water molecules. Each $Zn(II)$ center is hexa-coordinated with a distorted octahedral coordination geometry supplied by two carboxylate oxygen atoms from one 3,4-Pybz ligand, two nitrogen atoms from two different 3,4-Pybz ligands and two oxygen atoms from two coordinated water molecules. The $Zn(1)—O_{\text{carboxylate}}$ bonds (2.175(4) and 2.194(4) Å) are slightly longer than the $Zn—O_{\text{water}}$ bonds (1.997(4) and 2.109(4) Å). This may be due to the fact that the carboxylate group in the bidentate chelating mode weakens the $Zn—O$ bonding interactions. All $Zn—O$ distances (from 1.997(4) to 2.194(4) Å) and $Zn—N$ distances (from 2.100(4) to 2.305(5) Å) fall in the normal range. 3,4-Pybz ligands in complex **I** display two kinds of coordination modes:



Scheme 1.

One mode connects one $Zn(II)$ center via pyridyl-N atom; the other chelates one $Zn(II)$ center via the carboxylate group in the bidentate chelating mode and bridges another $Zn(II)$ center via one pyridyl-N atom. Based on such coordination modes of L ligands, an infinite 1D chain was formed (Fig. 1b), such adjacent 1D chains are connected into a 2D layer via $O(2w)–H(4w)···O(3)$ hydrogen-bonding interaction between the deprotonated carboxylate O atoms and the coordinated water molecules (Fig. 1c). The 2D layers are further extended into 3D supramolecular net via $O—H···O$ hydrogen-bonding interactions ($O(2w)–H(3w)···O(4)$, $O(1w)–H(2w)···O(3)$, and $O(1w)–H(1w)···O(2)$) among the occupied and unoccupied carboxylate O atoms and the coordinated water molecules (Fig. 1d).

Table 1. Crystallographic data and refinement parameters for structures **I** and **II**

Parameter	Value	
	I	II
Empirical formula	C ₂₄ H ₂₉ N ₂ O ₆ Zn	C ₂₄ H ₁₇ N ₂ O ₄ Ag
Formula weight	497.79	505.27
Crystal size, mm	0.42 × 0.39 × 0.21	0.30 × 0.28 × 0.11
Crystal system	Triclinic	Triclinic
Space group	<i>P</i> 1	<i>P</i> 1̄
<i>a</i> , Å	6.0528(6)	8.2484(9)
<i>b</i> , Å	7.7930(4)	10.3371(11)
<i>c</i> , Å	11.6702(12)	12.2031(14)
α, deg	84.386(2)	89.588(2)
β, deg	75.8830(10)	87.0870(10)
γ, deg	84.801(2)	70.9240(10)
<i>V</i> , Å ³	530.02(8)	982.03(19)
ρ _{calcd} , mg/cm ³	1.560	1.709
<i>Z</i>	1	2
<i>F</i> (000)	256	508
Absorption coefficient, mm ⁻¹	1.204	1.062
Max and min transmission	0.7861 and 0.6317	0.8921 and 0.7411
θ Range for data collection, deg	2.63–25.00	2.62–25.00
Limiting indices	−6 ≤ <i>h</i> ≤ 7, −9 ≤ <i>k</i> ≤ 9, −13 ≤ <i>l</i> ≤ 12	−9 ≤ <i>h</i> ≤ 9, −12 ≤ <i>k</i> ≤ 12, −14 ≤ <i>l</i> ≤ 10
Reflections collected/unique	2714/2207	5119/3400
Completeness to θ = 25.00, %	98.2	98.70
Data/restraints/parameters	2207/9/298	3400/0/283
GOOF	1.068	1.023
Final <i>R</i> indices (<i>I</i> > 2σ(<i>I</i>))	<i>R</i> ₁ = 0.0282, <i>wR</i> ₂ = 0.0650	<i>R</i> ₁ = 0.0389, <i>wR</i> ₂ = 0.0805
<i>R</i> indices (all data)	<i>R</i> ₁ = 0.0294, <i>wR</i> ₂ = 0.0657	<i>R</i> ₁ = 0.0644, <i>wR</i> ₂ = 0.0956

$$R_1 = \Sigma(|F_o| - |F_c|)/\Sigma|F_o|, wR_2 = [\Sigma w(|F_o|^2 - |F_c|^2)^2/\Sigma w(F_o)^2]^{1/2}.$$

Table 2. Geometric parameters of hydrogen bonds for complexes **I** and **II***

Contact D—H···A	Distance, Å			Angle D—H···A, deg
	D—H	H···A	D···A	
I				
O(2w)—H(4w)···O(3a)	0.85	1.95	2.793(6)	173
O(2w)—H(3w)···O(4b)	0.85	1.84	2.685(6)	171
O(1w)—H(2w)···O(3b)	0.85	1.76	2.613(5)	176
O(1w)—H(1w)···O(2c)	0.85	1.84	2.674(5)	165
II				
O(4)—H(4)···O(1)a	0.82	1.66	2.459(4)	164

* Symmetry codes: (a) *x*, *y* + 1, *z* − 1; (b) *x* + 1, *y* + 1, *z* − 1; (c) *x* + 1, *y*, *z* (I); (a) *x* − 1, *y* + 1, *z* (II).

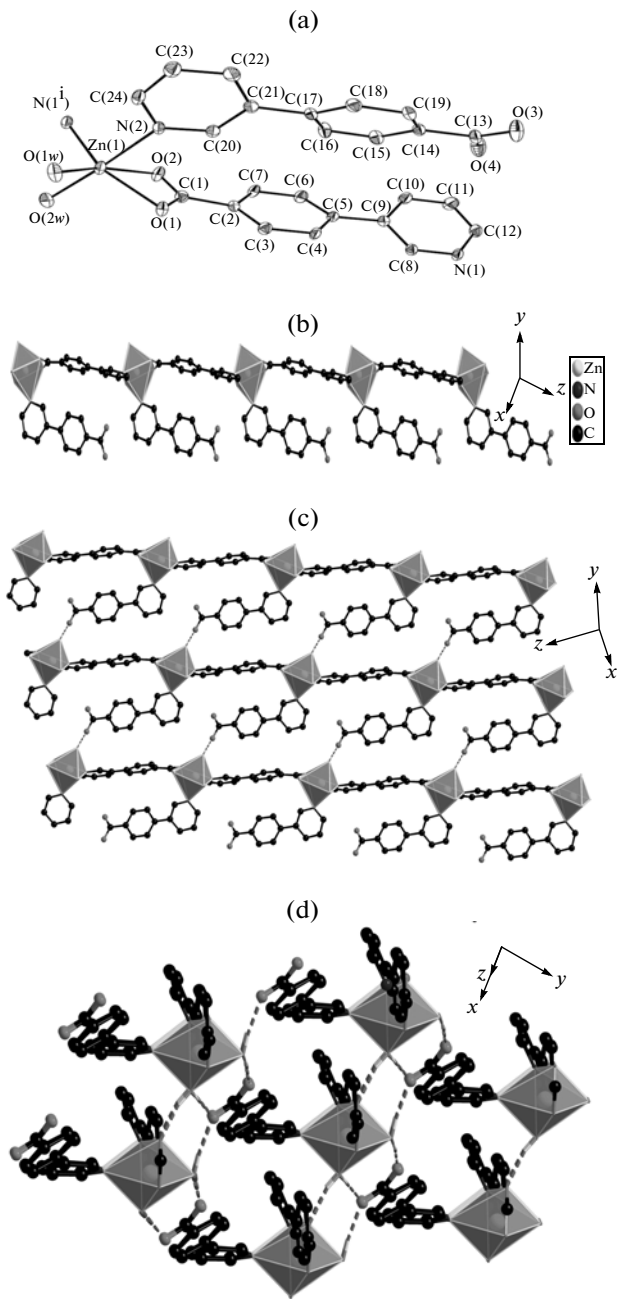


Fig. 1. Thermal ellipsoid plot of the asymmetry unit of **I** (30% probability ellipsoids). Symmetry code: $\mathbf{I} = x - 1, y, z + 1$ (a); an infinite chain in **I** (b); 2D sheet consisting of 1D chains linked by $\text{O}(2w)-\text{H}(4w)\cdots\text{O}(3)$ hydrogen-bonding interactions (c); 3D supramolecular structure formed by $\text{O}(2w)-\text{H}(3w)\cdots\text{O}(4)$, $\text{O}(1w)-\text{H}(2w)\cdots\text{O}(3)$, and $\text{O}(1w)-\text{H}(1w)\cdots\text{O}(2)$ (d). In (c) and (d), the hydrogen atoms not involved in forming hydrogen bonds are omitted for clarity.

Compound **II** has a 1D chain structure. As shown in Fig. 2a, there exist two types of coordination environments around the Ag ions in the crystal structure. Ag(1) ion is ligated with two nitrogen atoms ($\text{Ag}(1)-\text{N} 2.243(3)$ Å) and two carboxylate oxygen atoms

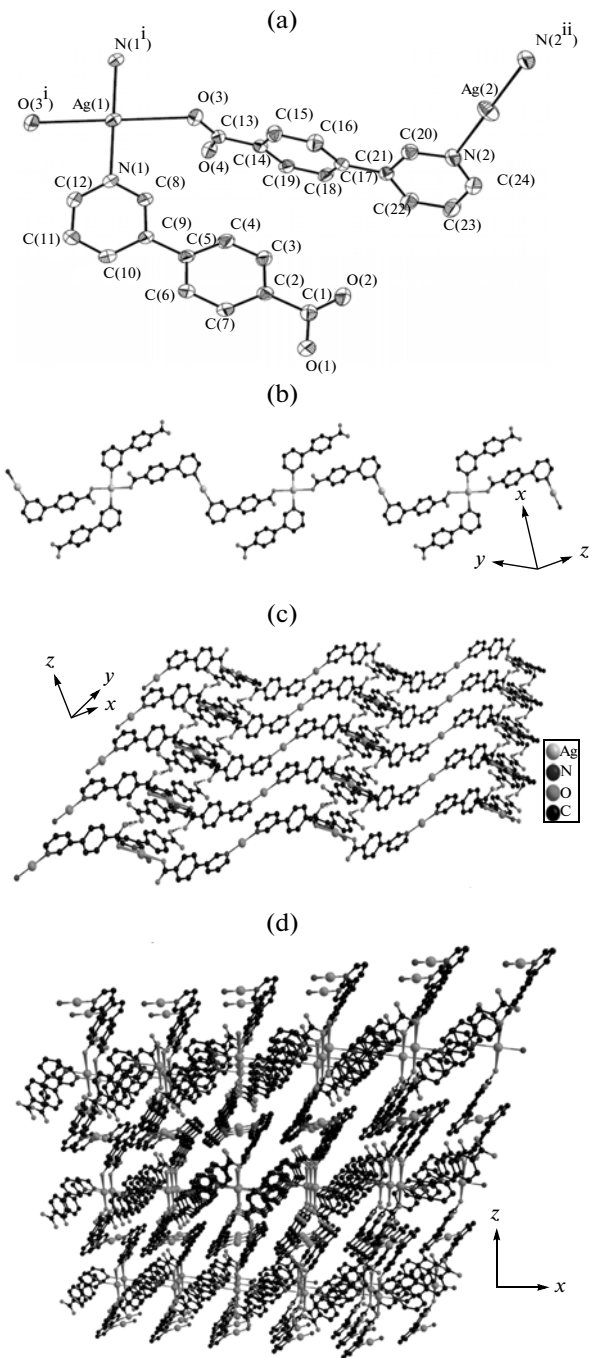


Fig. 2. The coordination environment of $\text{Ag}(1)$ and $\text{Ag}(2)$ in **II** (30% probability ellipsoids). Symmetry code: ${}^{\text{i}} -x, -y + 2, -z + 1; {}^{\text{ii}} -x, -y, -z + 2$ (a); an infinite chain with Ag1(I) and Ag2(I) centers arranged alternatively in **II** (b); a wavelike layer constructed via $\text{O}-\text{H}\cdots\text{O}$ hydrogen bonding interactions (c) (hydrogen atoms not involved in forming hydrogen bonds are omitted for clarity); 3D supramolecular structure formed by hydrogen bonding interactions and $\pi\cdots\pi$ stacking interactions (d).

($\text{Ag}(1)-\text{O} 2.634(3)$ Å) from four different 3,4-Pybz ligands, forming a distorted square planar coordination geometry. While each $\text{Ag}(2)$ ion is coordinated by

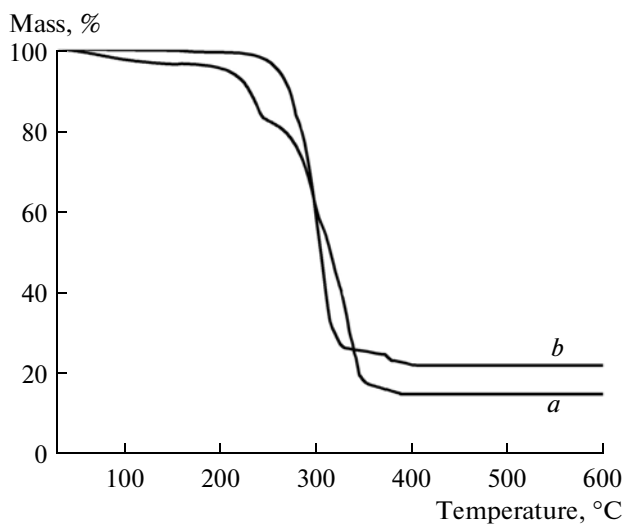


Fig. 3. The TGA curves of complexes **I** (a) and **II** (b).

two nitrogen atoms ($\text{Ag}(2)-\text{N}$ 2.181(4) Å) from two 3,4-Pybz ligands to furnish a linear coordination geometry. 3,4-Pybz ligands in complex **II** display two kinds of coordination modes (Scheme 1); one acts as terminal ligand to coordinate one $\text{Ag}(\text{I})$ center in monodentate; the other bridges two $\text{Ag}(\text{I})$ centers via one carboxylate O atom and one pyridyl-N atom. Thus, an infinite chain with $\text{Ag}(1)$ and $\text{Ag}(2)$ centers arranged alternatively was generated, in which the adjacent $\text{Ag}\cdots\text{Ag}$ distance is 11.966(4) Å (Fig. 2b). There are abundant weak interactions around $\text{Ag}(1)$ and $\text{Ag}(2)$, $\text{Ag}(1)\cdots\text{O}(1)$, $\text{Ag}(2)\cdots\text{O}(2)$, and $\text{Ag}(2)\cdots\text{O}(4)$ (2.913(4), 3.045(3), and 2.833(4) Å, respectively), which are shorter than the sums of the van der Waals radii of Ag and O (3.24 Å). The adjacent chains are connected into a wavelike layer via $\text{O}-\text{H}\cdots\text{O}$ hydrogen bonding interactions (Fig. 2c), which combine with $\pi\cdots\pi$ stacking interactions (the shortest centroid–centroid distance between parallel benzene and pyridyl rings of the 3,4-Pybz ligands is 3.36(9) Å and the shortest centroid–centroid distance between parallel pyridyl rings is 3.841(3) Å) contribute to the formation of a 3D supramolecular network (Fig. 2d).

The absorption band at 3242 cm^{-1} for **I** indicates the presence of the water molecules, while the characteristic peaks at 1589, 1537 and 1409, 1373 cm^{-1} for **I**, 1592 and 1433, 1340 cm^{-1} for **II**, are associated with the asymmetric (COO) and symmetric (COO) stretching vibrations. The peak at 1695 cm^{-1} for **I** is characteristic of free carboxyl groups.

TGA of compounds **I** and **II** were performed in a N_2 atmosphere when the samples were heated to 600°C at a constant rate of $10^\circ\text{C}/\text{min}$. The TG curves are depicted in Fig. 3. For complex **I**, the initial mass loss of 7.16% from 63 to 201°C is attributed to the departure of two water molecules (calcd. 7.23%), whereas the release of 3,4-Pybz ligand molecules occurred

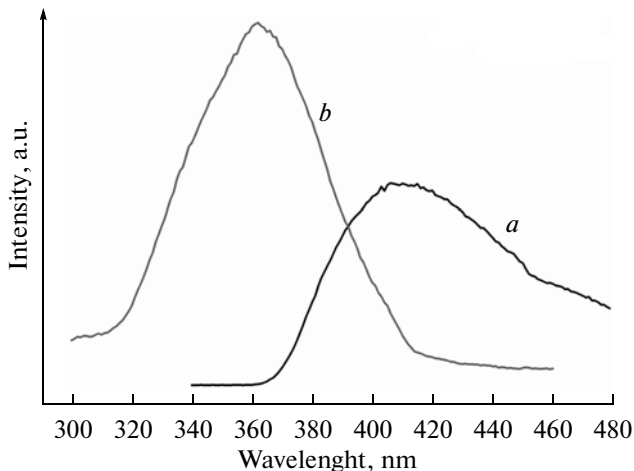


Fig. 4. Solid-state emission spectra of **I** (a) and **II** (b) at room temperature.

from 209 to 394°C . Complex **II** shows thermal stability as no strictly clean weight loss step occurs below 253°C . The weight-loss step occurs above 291 and 253°C which corresponds to the decomposition of frameworks and the residue accounts for 21.9%, which is nearly in agreement with the calculated value of 18.9%, by assuming the final product is Ag.

Due to the fact that coordination polymers are able to adjust the emission wavelength of organic ligands via incorporation of metal atoms, it is quite of importance to investigate the luminescence properties of coordination polymers in view of potential applications as light-emitting diodes [14]. The photoluminescence of **I** and **II** were investigated in the solid state at room temperature. As indicated in Fig. 4, the emission spectra of complexes **I** and **II** exhibit strong emission. The emission maxima (λ_{em}) are 406 nm (**I**) and 362 nm (**II**) ($\lambda_{\text{ex}} = 330\text{ nm}$ for **I**, 270 nm for **II**), respectively. Compared with the case of the free ligand 3,4-HPybz with maximum emission peak at 387 nm ($\lambda_{\text{ex}} = 327\text{ nm}$) reported previously [9], the maximal emission of **I** may be attributed to the ligand-centered transitions [9]. The blue shift of the luminescence of **II** compared to that of the free ligand may originate from the coordination effect of the ligand to the silver ions [15].

ACKNOWLEDGMENTS

The work was supported by the National Marine Public Welfare Projects (grant no. 2000905021), the Guangdong Oceanic Fisheries Technology Promotion Project (grant no. A2009003–018(c)), the Guangdong Chinese Academy of Science comprehensive strategic cooperation project (grant no. 2009B091300121), the Guangdong Province key project in the field of social development (grant no. A2009011–007(c)), the Science and Technology Department of Guangdong

Province Project (grant no. 00087061110314018) and the Guangdong Natural Science Fundation (no. 9252408801000002).

REFERENCES

1. Qiu, S. and Zhu, G., *Coord. Chem. Rev.*, 2009, vol. 253, p. 2891.
2. Ma, L., Abney, C., and Lin, W., *Chem. Soc. Rev.*, 2009, vol. 38, p. 1248.
3. Allendorf, M.D., Bauer, C.A., Bhakta, R.K., and Houk, R.J.T., *Chem. Soc. Rev.*, 2009, vol. 38, p. 1330.
4. Zhou, G.J. and Wong, W.Y., *Chem. Soc. Rev.*, 2011, vol. 40, p. 2541.
5. Carlucci, L., Ciani, G., and Proserpio, D.M., *Coord. Chem. Rev.*, 2003, vol. 246, p. 247.
6. Zhong, R.Q., Zou, R.Q., Du, M., et al., *CrystEngComm*, 2008, vol. 10, p. 605.
7. Zhang, Y.B., Zhou, H.L., He, C.T., et al., *Chem. J. Chin. Univ.*, 2011, vol. 324, p. 97.
8. Fang, W.H., Wang, Z.L., and Yang, G.Y., *Chin. J. Inorg. Chem.*, 2010, vol. 26, p. 1917.
9. Jiang, X.J., Du, M., Sun, Y., et al., *J. Solid. State Chem.*, 2009, vol. 182, p. 3211.
10. Guo, F., *Z. Anorg. Allg. Chem.*, 2010, vol. 636, p. 857.
11. Zhang, X.M., Jing, X.H., and Gao, E.Q., *Inorg. Chim. Acta*, 2011, vol. 365, p. 240.
12. SMART, SAINT, and SADABS, Madison (WI, USA): Bruker AXS Inc., 2007.
13. Sheldrick, G.M., *Acta Crystallogr. A*, 2008, vol. 64, p. 112.
14. Seward, C., Jia, W.L., Wang, H.Y., et al., *Angew. Chem. Int. Ed.*, 2004, vol. 43, p. 2933.
15. Shu, M.S., Tu, C.L., Xu, W.D., et al., *Cryst. Growth Des.*, 2006, vol. 6, p. 1890.